NIH-PA Author Manuscript

An implantable bolus infusion pump for use in freely moving, nontethered rats

D. P. HOLSCHNEIDER[1,2,4], **J.-M. I. MAAREK**[3], **J. HARIMOTO**[3], **J. YANG**[1], and **O. U. SCREMIN**[4,5]

[1]Department of Psychiatry and the Behavioral Sciences, University of Southern California School of Medicine, Los Angeles 90033

[2]Department of Neurology, University of Southern California School of Medicine, Los Angeles 90033

[3]Department of Biomedical Engineering, University of Southern California School of Engineering, Los Angeles 90089

[4]Greater Los Angeles Veterans Affairs Healthcare System, Los Angeles 90073

[5]Department of Physiology, University of California at Los Angeles School of Medicine, Los Angeles, California 90095

Abstract

One of the current constraints on functional neuroimaging in animals is that to avoid movement artifacts during data acquisition, subjects need to be immobilized, sedated, or anesthetized. Such measures limit the behaviors that can be examined, and introduce the additional variables of stress or anesthetic agents that may confound meaningful interpretation. This study provides a description of the design and characteristics of a self-contained, implantable microbolus infusion pump (MIP) that allows triggering of a bolus injection at a distance in conscious, behaving rats that are not restrained or tethered. The MIP is externally triggered by a pulse of infrared light and allows in vivo bolus drug delivery. We describe application of this technology to the intravenous bolus delivery of iodo[^{14}C]antipyrine in a freely moving animal, followed immediately by lethal injection, rapid removal of the brain, and analysis of regional cerebral blood flow tissue radioactivity with the use of autoradiography. The ability to investigate changes in brain activation in nonrestrained animals makes the MIP a powerful tool for evaluation of complex behaviors.

Keywords

drug delivery; functional neuroimaging; cerebral blood flow; iodo-antipyrine; autoradiography

One of the dilemmas facing functional neuroimaging is that subjects need to be largely immobilized to avoid movement artifact during data acquisition. In animals, functional neuroimaging with the use of quantitative autoradiography, $H_2^{15}O$-positron emission

tomography, or functional magnetic resonance imaging is mostly performed on immobilized or anesthetized subjects. Such measures limit the behaviors that can be examined and introduce the additional variables of stress or anesthetic agents that may confound interpretation. Thus many fundamental mammalian behaviors, such as aggression, mating, feeding, and fear, have remained largely unstudied. New techniques are acutely needed to provide a more naturalistic assessment of the neural mechanisms underlying such complex behaviors.

Currently available technology does not permit bolus infusion of radiotracers in conscious, behaving, non-tethered small animals. Commercially available continuous infusion pumps cannot be used for functional neuroimaging because their slow infusion rates result in nonspecific distribution of the tracer. Rapid delivery of a radiotracer in tethered animals connected to an external pump through a transcutaneous body port (4) is practical only in the study of behaviors of animals in isolation and is limited to behaviors that present a low risk of entanglement of the animal with its catheter. The extent to which the stress of tethering reshapes "normal" behavior in these paradigms is likely substantial.

We have developed a self-contained, implantable microbolus infusion pump (MIP) for bolus injection in conscious, freely moving rats. The MIP can deliver a bolus of radiotracer in vivo, thus enabling a naturalistic assessment of brain activation during complex behaviors. In this study, we describe the design of the MIP and an application in which the MIP is used to image cerebral blood flow (CBF) tracer distribution in freely moving, nontethered animals.

MATERIALS AND METHODS

Overview

The MIP was assembled using a modular design. Figure 1 depicts a reservoir (no. 1) covered by an elastomeric disk, which created a hydraulic pressure source to force liquid out of the MIP at a constant flow rate. In the "off" state, flow was blocked by a solenoid microvalve (no. 7) inside a separate electronics module (no. 4). On being transcutaneously illuminated by infrared (IR) light, a phototransistor (no. 5) in the electronics module opened the microvalve. The elastomeric reservoir pushed the content of a coiled ejection chamber (no. 2) out through an intravenous catheter. For functional neuroimaging with a radiotracer, opening of the valve first released the radiotracer contained in the ejection chamber into the animal's circulation, and, after a delay of several seconds, injected a euthanasia solution placed in the reservoir. The MIP weighed 34 ± 2 g (~10% of body wt).

Fabrication of MIP

Reservoir—The reservoir (25 mm diameter × 6.6 mm height, dead vol 0.1 ml, total vol 1.1 ml) was made of a stainless steel housing with a medical-grade silicone cover that acted as an elastomeric disk spring (outlet pressure ~124 mmHg). The reservoir was customized from a commercially available infusion pump (Esox Technology; Eagan, MN) by removing the flow restrictor, which normally limits the flow rate for slow infusion applications. The

reservoir was designed for a constant flow release of its content that is insensitive to changes in ambient temperature, pressure or fibrous encapsulation (18).

Electronic module—The electronic module (Fig. 1*C*) consisted of a microvalve, a photosensor transistor used as a switch to trigger the valve, circuitry to hold the valve open after it has been triggered, and a battery power source. A 12-V stainless steel solenoid valve (Lee; Essex, CT) was chosen because of its small size and weight (2 g), its ability to provide high hydraulic flows (flow resistance = 3.34×10^5 g/s·cm^4), and its low power consumption (250 mW to hold open, nominal). Remote triggering of the MIP was elicited by transcutaneous illumination of a silicone photodarlington sensor (model SD1410-001, Honeywell; Morristown, NJ) with peak sensitivity in the near infrared spectrum (880 nm). Illumination of the photosensor produced a photocurrent, which activated a silicone-controlled rectifier switch (model MCR 100, On Semiconductor; Phoenix, AZ). Current from the battery power source flowed through a red light-emitting diode (model 604-L934S, Kingbright; City of Industry, CA), the silicone-controlled rectifier and the microvalve circuitry to open the hydraulic channel in the valve. Light from the red light-emitting diode was visible through the animal's skin to give visual feedback on the status of the microvalve. The MIP was turned off by the passage of a magnet over the skin overlying the implant, thereby activating a REED switch (model KSK-1C29–1525, Meder Electronics; Mashpee, MA), which interrupted the electric circuit and closed the valve. The circuit was powered by four 3-V lithium batteries. All of the components of the electronic module were soldered on a printed circuit board.

Encapsulation of the electronic module—Two segments of Silastic tubing (1.65 mm OD, 0.76 mm ID) were inserted to connect the valve to the reservoir and the ejection chamber. The electronics module was then embedded in optically clear silicone for waterproofing and electrical insulation. The silicone and its catalyst were thoroughly mixed and placed in a vacuum chamber for 20 min to remove air bubbles. The printed circuit board was laid in a polyurethane mold that was slowly filled with silicone. The silicone cured overnight at room temperature to a rubbery strength (Durometer Shore A30).

Ejection chamber—The elliptical ejection chamber was fabricated of polyethylene tubing (1.9 mm OD, 1.4 mm ID, 34 cm length, 521 µl volume) flattened into a coil and stabilized with a 1-mm layer of silicone. The ejection chamber was fixed to the bottom of the encapsulated electronic module with a thin rim of silicone.

Intravenous access port—The coiled ejection chamber connected to a heparin-coated polyurethane catheter (7.0 cm, 1.19 mm OD, 0.69 mm ID, model CBAS-C35, Instech Laboratories; Plymouth Meeting, PA), which provided access to the animal's external jugular vein. Placed between the ejection chamber and the catheter was a T tube connector (Small Parts; Miami Lakes, FL) leading to a Silastic tube, which allowed for percutaneous access to the implanted pump.

Implantation of MIP

Presurgical preparation of MIP—The intravenous catheter was sterilized with the use of ethylene oxide. The MIP was sterilized in 2.65% glutaraldehyde solution overnight, after which it was thoroughly rinsed with sterile water. The reservoir chamber was sterilized by steam (121°C, 20 min), per the manufacturer's specifications. All infusates were filtered through a 0.2-μm syringe filter. With the use of an aseptic technique, the outflow tubing of the reservoir was connected, first to the ejection chamber by a stainless steel connector (19 gauge, 1.5 cm length), then to the T tube, and finally to the inflow of the solenoid valve.

Anesthesia—Experiments were conducted on adult male Sprague-Dawley rats (325–350 g, Harlan Sprague Dawley). The rats were anesthetized with halothane (2.5% induction, 1.3% maintenance) in a mixture of 30% O_2-70% N_2. Body temperature was maintained at 37.0°C with a homeothermic water blanket connected to a temperature controller (model TCAT-12, Physitemp; Clifton, NJ). All surgery was performed under standard fluorescent ceiling lights to which the photosensor was relatively insensitive. The aseptic technique was followed during all aspects of the animal's surgery. All procedures performed were reviewed and approved by the institutional animal care and use committee.

Cannulation of external jugular vein—A 2 cm × 4 cm area on the ventromedial aspect of the neck was shaved and a 1-cm longitudinal skin incision was made ventrally, lateral to the midline of the neck. The right external jugular vein was separated from the surrounding neck musculature. The jugular vein was occluded with a microaneurysm clip and the venous catheter was inserted and advanced 4.0 cm caudally into the right atrium. The catheter was fixed with two 5-0 silk ligatures, tunneled subcutaneously onto the dorsum of the neck, and linked to the distal port of the percutaneous T tube connector. A single dose of the antibiotic ampicillin (200 mg/kg iv) was administered intraoperatively.

Subcutaneous implantation of MIP—A 3 cm × 6 cm area was shaved on the dorsum of the rat at the level of scapula. A 4-cm skin incision was made along the dorsal midline from the scapula to the center of the back. A pouch was formed on both sides by separating the skin from the underlying tissue by blunt dissection. The MIP was inserted with its photosensor facing upward and anchored by suturing the overlying fascia to four O-ring eyelets embedded on the lateral aspects of the electronic module. The outflow of the ejection chamber was connected to the proximal port of the T tube connector. The skin incision was closed with 2-0 silk sutures, except for a small hole, which allowed the tubing arising from the stem of the T tube connector to pass through the skin. This tubing was sealed at its end with a stainless steel plug.

Postoperative care—After discontinuation of the anesthesia, the rats were placed in a warm environment and allowed to recover. Animals were housed singly in the vivarium under standard ceiling fluorescent lighting, with a 12:12-h light/dark cycle (7:00 AM to 7:00 PM). Catheter patency was maintained by daily flushes through the T tube connector of 0.8 ml of 0.9% saline, followed by a 0.15-ml flush of 0.9% saline-50 U/ml heparin.

Characterization of MIP Performance

In vivo triggering distance—The ability of an IR light source (an array of 160 light emitting diodes with wavelengths at 850 and 880 nm, MCM Electronics; Centerville, OH) to trigger the MIP was examined by mounting the lamp on a movable gantry above the animal preparation. This allowed us to define the maximum distance at which the implanted MIP could be triggered with the light held vertically above the MIP or at a 60° angle off of the vertical. To examine the effect of skin pigmentation, a comparison was made between albino Sprague-Dawley rats ($n = 8$) and ACI/SegHsd Black Agouti rats ($n = 2$).

Infusion pressure—Changes in the infusion pressure during discharge of the MIP were recorded both ex vivo and in vivo in the anesthetized rat by connecting the pump through its percutaneous T tube to a Statham strain-gauge pressure transducer. The reservoir was filled with 1.0 ml of saline solution with a 30-gauge needle, and the MIP was triggered with an IR light source. The pressure signal at the site of the T tube was digitized (sampling rate 40 Hz) during the emptying of the reservoir and recorded online (Axotape 2.0, Axon Instruments; Foster City, CA).

Flow rate—The ex vivo flow rate (μl/s) of the pump was quantified by measuring changes in the reservoir weight as a function of time. A bipolar junction transistor (2N 3904) replaced the silicone-controlled rectifier in the electronic circuit, such that the circuit remained activated only during illumination of the photosensor. The reservoir was placed on a Sartorius A120S electronic balance. Activation of the valve occurred in 0.8-s intervals with an electronically controlled light source.

Evaluation of euthanasia—The time required for a euthanasia agent (pentobarbital 50 mg/kg and 3 M KCl) to elicit cardiac arrest after triggering of the pump was evaluated in a rat anesthetized as described above. Two platinum needle electrodes were inserted in the subcutaneous tissue overlying the right scapula and the apex of the heart to record the electrocardiogram. The femoral artery was cannulated with a polyethylene-50 catheter and arterial blood pressure was measured with a Statham pressure transducer. Data were digitized (sampling rate 400 Hz) and recorded using the Axotape 2.0 signal recording system. The reservoir was loaded with 1.0 ml of the euthanasia solution, and the pump was triggered by exposure to the IR light source.

Assessment of CBF Tracer Distribution

Loading of the radioactive tracer—The rat was placed in a disposable rodent restrainer (Decapicone; Kent Scientific). A 2 cm × 2 cm window was cut through the flexible plastic overlying the percutaneous T tube and subcutaneous reservoir. With the valve kept in the closed position, the ejection chamber of the MIP was back loaded through the T tube connector with the radiotracer, iodo[14C]antipyrine (100 μCi/kg in 300 μl of 0.9% saline; Amersham Biosciences; Piscataway, NJ). The radiotracer was preceded and followed by slow loading of a 50-μl air spacer, which maintained the tracer separate from the euthanasia solution in the reservoir and the saline solution immediately posterior to the valve. The animal was removed from the restraining device and placed in an experimental cage.

In vivo injection of radiotracer—Experiments were performed in a 2 m × 1 m × 1 m box lined with acoustic tile. The box housed an animal behavioral cage (30 cm × 30 cm × 50 cm), whose ceiling was constructed of a clear Plexiglas mesh. Background noise intensity inside the behavioral cage was measured with a sound meter at 52 dB (Radio Shack; Fort Worth, TX). Four IR light sources, each consisting of an array of 160 light-emitting diodes of wavelengths 850 and 880 nm (MCM Electronics) illuminated the cage interior from above. A computer program written in LabVIEW (National Instruments; Austin, TX) toggled a digital output port (model DT7100, Data Translation; Marlboro, MA) to energize a solid-state relay and turn on the IR lights. Activity inside the cage during illumination was monitored from outside the experimental chamber by video camera. After the radiotracer was loaded, the animals were allowed to freely explore the darkened chamber for 40 min, after which the IR lights automatically turned on. The triggering of the pump allowed for bolus injection of iodo[14C]antipyrine, followed immediately by injection of the euthanasia solution, with resultant cardiac arrest, termination of brain perfusion, and death. The brains of the animals were rapidly removed, flash-frozen in methyl-butane at −70°C, embedded in OCT compound (Miles; Elkhart, IN), and stored at −70°C.

Autoradiography—Cerebral cortical blood flow was measured as previously described in immobilized animals (10, 11, 16, 17). Brains were cut in a cryostat at −20°C in 20-μm-thick coronal sections, heat-dried on glass slides, and exposed for 2 wk at room temperature to Kodak Ektascan films in spring-loaded X-ray cassettes along with 16 radioactive [14C] standards (American Radiolabeled Chemicals; St. Louis, MO). Autoradiographs of brain sections were digitized and brain regions identified with an anatomic atlas of the rat brain (15), and were then transcribed to a visual template. An overlay of this template onto the digitized images allowed measurement of the optical density of locations in the cortical mantle in a manner invariant between animals. The optical density of locations in the cortical mantle was measured with Image Pro Plus software (version 4.0, Media Cybernetics; Silver Spring, MD). Quantification of optical density of autoradiographs and comparison with that induced by standards of known radioactivity allowed determination of [14C] regional tissue radioactivity.

Analysis of tissue radioactivity data—Measurements of regional tissue radioactivity was performed for each animal in 246 cortical regions and distributed in 13 coronal planes (antipyrine, +2.7, +1.6, −0.3, −0.8, −1.3, −1.8, −3.3, −4.3, −5.3, −5.8, −6.3, −7.3, and −8.3 mm anterior to bregma). These regions were sampled in both hemispheres and averaged. A Z-transformation was performed on the tissue radioactivity data to produce patterns of regional tracer concentrations for each animal (12). This transformation has been routinely employed in the analysis of positron emission tomography maps because it introduces minimal dependence on absolute tracer activity when the number of locations studied is large (5). Abstraction of the tracer distribution pattern by this procedure eliminates variations in mean tracer distribution between subjects and experimental groups created by global effects on vascular smooth muscle and systematic experimental error. This is an advantage when studying patterns, but it precludes assessment of absolute CBF. Group mean Z-scores were calculated for each brain region and displayed as topographical maps for the dorsal, lateral, and basal cortical surfaces of the brain. In these two-dimensional maps

(Fig. 5), the *x*- and *y*-coordinates are obtained from measures of the anatomical distances within the autoradiographs. To avoid discontinuities in the graphic representation, the space between our 13 coronal brain slices and 16–20 locations within each slice where there were no measurements was filled with values calculated by a standard linear interpolation.

RESULTS

After fabrication, pumps were immersed in water for 1 wk to screen out waterproofing failures. The failure rate at 1 wk before implantation was <5%, and thereafter, for the duration of the experiment was essentially zero. Empirically, we found that the MIP functioned properly with the valve continuously energized for 45 min on a new set of batteries. The MIP could be reimplanted for a total of three times before the batteries had to be replaced.

There was no evidence of interference with the implant by animals, during the 3-day recovery period as evidenced by an absence of cutaneous scratches or bleeding. Subcutaneous implantation of the MIP showed a small amount of clear exudate in 20% of implants. No erythema, ulceration, or pus was seen on postmortem autopsy at postoperative *day 3*. At the time of animal death, the tips of all catheters were consistently located in the right atrium. Visual inspection revealed no signs of catheter thrombosis, tissue ingrowth, or debris.

Sensitivity of implanted MIP to triggering

Under conventional laboratory fluorescent illumination the pump remained in its inactive state. Transcutaneous triggering of the pump with our IR light source was induced at a maximum vertical distance of 66 ± 2 cm (means $\pm$ SE, $n = 8$). Despite the narrow acceptance angle of the photodarlington (20°), scattering of the IR light by the skin and underlying tissue allowed triggering of the pump at a maximum distance of 41 ± 3 cm when the lamp was 60° off of the vertical. In albino rats, triggering of the subcutaneous sensor was equally effective, independent of the presence or absence of hair, a finding that allowed the MIP to be used independently of hair regrowth in the implanted animals. This is likely due to the reflection and diffusion of impinging light that allows transmission of the IR signal without significant absorption by the albino hair and skin. In Black Agouti rats, skin pigmentation of the shaved skin produced little change in the ability of our IR light to trigger the sensor. However, the presence of the black-pigmented hair in these animals increased light absorption, thereby decreasing the trigger distance by 80%.

Pressure profiles and flow rate

The pressure profile of the MIP at the outflow of the distal catheter in the ex vivo state (Fig. 2*A*) was characterized by three phases: *1*) initial drop, *2*) plateau, and *3*) gradual decline. The initial drop was brief in duration (~120 ms) and resulted in pressure change from ~124 to ~36 mmHg. The plateau phase lasted ~4.0 s during which the pressure remained at 34–35 mmHg. The small pressure variations observed during the plateau reflected the varying compliance of the elastomeric disk reservoir as a function of the reservoir volume (6). A more gradual decline in the pressure to ~0 mmHg over the next 4.0 s reflected the decrease

in the spring constant of the Silastic disk reservoir as it approached its resting position. A similar pressure profile was seen for the MIP in the in vivo state (Fig. 2*B*). Of note, the in vivo plateau pressures were higher (~41–44 mmHg) and more variable from animal to animal than the plateau pressures observed ex vivo. Baseline pressures after discharge of the reservoir remained at ~3–4 mmHg. These differences likely reflected the rat central venous pressure downstream from MIP in the in vivo experiments. The MIP flow rate ex vivo (Fig. 2*C*) also showed the initial drop, plateau, and gradual decline phases. Flow rates varied from ~180 to 65 μl/s during the pump discharge.

In vivo administration of radiotracer and euthanasia agent

Injection of the radiolabeled tracer was followed immediately by lethal injection. Effects of the euthanasia agent were apparent at ~8 s after the pump was triggered (Fig. 3). This resulted in cardiac arrest, a precipitous fall of arterial blood pressure, termination of brain perfusion, and death.

Assessment of CBF

A representative autoradiograph depicting regional CBF-related tracer distribution in two coronal sections is presented in Fig. 4. Rats revealed their highest regional Z-scores of CBF-related tracer distribution (Fig. 5) in a zone that included the whole extension of the parietal cortex. An additional cluster of locations with high regional Z-scores was also found in the anterior-medial aspects of the temporal cortex and anterior-lateral portions of the occipital cortex. The lowest regional Z-scores were seen in the amygdala, entorhinal, posterior perirhinal, posterior piriform, and retrosplenial cortex.

DISCUSSION

The device reported in this study is a self-contained, implantable pump capable of bolus delivery of a pharmacological agent by remote activation in small animals that are neither restrained nor tethered. These characteristics make it a unique device for experimental studies that cannot be achieved with currently available slow-infusion pumps. The current study demonstrates a novel application of the MIP for imaging of CBF tracer distribution in freely moving rats. Topographical maps of regional CBF tracer distribution revealed increased blood flow in parietal cortex and anterior portions of temporal and occipital cortex. Lower regional blood flow was seen in the amygdala, entorhinal, posterior piriform, and perirhinal cortex. This topographical pattern was similar to that described previously in the unanesthetized restrained rat (11, 17).

The ability to administer radiotracers by remote activation to conscious, freely moving animals is a useful experimental technique in neuroimaging studies that seek to examine functional brain activation during behaviors that would otherwise be extinguished or modified by physical restraint of the animal. The brief time period between injection of the tracer and euthanasia allows excellent time resolution (<12 s) and a near-instantaneous view of tracer activity in the brain with minimal nonspecific diffusion. The high-spatial resolution of the autoradiograph (0.1 mm) allows detailed mapping of regional changes of tracer distribution. Because of the wide use of rodents as experimental models, the proposed

device should find broad applications in the neuroimaging of complex behaviors, although future work will need to evaluate the effect such an implant itself may have on reshaping behaviors.

Compartmentalization of the MIP into a reservoir module, electronic module, and ejection chamber has a number of advantages. Placement of all electronics in a single silicone encapsulation aids in the electrical insulation. Compartmentalization of the coiled ejection chamber containing the radiotracer allows for easy excision of this module from the implant after euthanasia of the animal. This is of particular utility in the decontamination of the pump for reuse. The ability to load the tracer externally through a percutaneous port on the day of the experiment, rather than during pump implantation, eliminates the need for daily radiation safety monitoring within the vivarium where animals are housed postoperatively.

Use of the near IR light to trigger the MIP has several advantages. First, the skin is semitransparent to light of this wavelength, with an "optical window" existing between ~700 and 950 nm, within which the absorption of light by melanin, hemoglobin, keratin, water, and other substances is relatively small (1), and the effects of scattering are reduced (2). Second, triggering the MIP with IR light is behaviorally noninvasive in rodents, which are largely insensitive to these wavelengths (14). Third, the sensitivity of the circuit can be adjusted to avoid triggering of the valve under fluorescent light, which contains only small amounts of energy in the IR spectrum. This allows the pump to be assembled and implanted under standard laboratory fluorescent illumination. With a silicone-controlled rectifier in a series with the solenoid valve, the latter remains open once the photosensor is illuminated by IR light, even if the animal moves away from the light source. This latched opening of the valve allows for complete, continuous delivery of the radiotracer independent of changes in the animal's body position. Because of the large pressure head delivered by the reservoir (outlet pressure ~124 mmHg) compared with the relatively low central venous pressure of the rat (~4 mmHg), small changes in the central venous pressure due to positional changes of the animal do not significantly change the flow rate. Though other means of triggering the pump are feasible (e.g., radio frequency), the choice of IR light was made because of the ready availability of commercial components that could easily be assembled for this application.

The current device should find applications not only in the field of neuroimaging but also in the fields of behavioral pharmacology and physiology. It is well known that the presence or absence of stress may substantially change an animal's behavior. Even minor routine handling procedures can induce a marked stress in animals, although the animal has been trained to this procedure and looks quiet (13). Handling an animal or drug injection by needle may suppress many behaviors at the time of occurrence such as aggression, sleep, and mating. Hence, the MIP promises useful application in the study of the effects of pharmacological agents on animal behaviors sensitive to interference by handling. Handling stress associated with drug injection by needle may also substantially change an animal's physiological response, as well as endocrine and metabolic parameters (3, 7–9). Use of the MIP promises to be a powerful tool in the minimally invasive study of the acute effects of pharmacological agents on physiological parameters. As such, the MIP represents a complementary technology to existing telemetry systems (i.e., Datasciences International;

St. Paul, MN) used in the assessment of brain electrical activity, cardiovascular parameters, temperature, and circadian rhythms.

In summary, no device exists that allows acute bolus drug administration to small animals in the nontethered, freely behaving state. The device we developed is self-contained, fully implantable, and can be triggered transcutaneously at a distance by IR light. Because of the wide use of rodents as experimental models, the proposed device should find broad applications in the fields of neuroimaging, as well as behavioral pharmacology and physiology.

Acknowledgments

References

1. Anderson RR, Parrish JA. The optics of human skin. J Invest Dermatol. 1981; 77:13–19. [PubMed: 7252245]

2. Anderson, RR.; Hu, J.; Parrish, JA. Optical radiation transfer in the human skin and application in in-vivo remittance spectroscopy. In: Marks, R.; Payne, PA., editors. Bioengineering and the Skin. Boston, MA: MTP; 1981. p. 253-265.

3. Benedek G, Szikszay M, Obal F. Stress-related changes of opiate sensitivity in thermoregulation. Life Sci. 1983; 33(Suppl 1):591–593. [PubMed: 6686639]

4. Bryan RM Jr. A method for measuring regional cerebral blood flow in freely moving, unstressed rats. J Neurosci Methods. 1986; 17:311–322. [PubMed: 3537542]

5. Clark C, Carson R, Kessler R, Margolin R, Buchsbaum M, DeLisi L, King C, Cohen R. Alternative statistical models for the examination of clinical positron emission tomography/fluorodeoxyglucose data. J Cereb Blood Flow Metab. 1985; 5:142–150. [PubMed: 3871782]

6. Cress AS, Wigness BD, Dorman FD, Rohde TD, Buchwald H. Portable data acquisition and control apparatus for implanted drug infusion pump interrogation. ASAIO J. 1993; 39:M695–M698. [PubMed: 8268627]

7. Euker JS, Meites J, Riegle GD. Effects of acute stress on serum LH and prolactin in intact, castrate and dexamethasone-treated male rats. Endocrinology. 1975; 96:85–92. [PubMed: 1109906]

8. Feenstra MG, Botterblom MH. Rapid sampling of extracellular dopamine in the rat prefrontal cortex during food consumption, handling and exposure to novelty. Brain Res. 1996; 742:17–24. [PubMed: 9117391]

9. Gartner K, Buttner D, Dohler K, Friedel R, Lindena J, Trautschold I. Stress response of rats to handling and experimental procedures. Lab Anim. 1980; 14:267–274. [PubMed: 7191933]

10. Goldman H, Sapirstein LA. Brain blood flow in the conscious and anesthetized rat. Am J Physiol. 1973; 224:122–126. [PubMed: 4566847]

11. Holschneider DP, Scremin OU. Effects of ovariectomy on cerebral flow of rats. Neuroendocrinology. 1998; 67:260–268. [PubMed: 9588695]

12. Holschneider DP, Scremin OU, Huynh L, Chen K, Seif I, Shih JC. Regional cerebral cortical activation in monoamine oxidase A-deficient mice: differential effects of chronic versus acute elevations in serotonin and norepinephrine. Neuroscience. 2000; 101:869–877. [PubMed: 11113335]

13. Le Maho Y, Karmann H, Briot D, Handrich Y, Robin JP, Mioskowski E, Cherel Y, Farni J. Stress in birds due to routine handling and a technique to avoid it. Am J Physiol Regul Integr Comp Physiol. 1992; 263:R775–R781.

14. Neitz J, Jacobs GH. Reexamination of spectral mechanisms in the rat (Rattus norvegicus). J Comp Psychol. 1986; 100:21–29. [PubMed: 3698578]

15. Paxinos, G.; Watson, C. The Rat Brain in Stereotaxic Coordinates. Sidney, Australia: Academic; 1986.

16. Sakurada O, Kennedy C, Jehle J, Brown JD, Carbin GL, Sokoloff L. Measurement of local cerebral blood flow with iodo[^{14}C]antipyrine. Am J Physiol Heart Circ Physiol. 1978; 234:H59–H66.

17. Scremin OU, Li MG, Scremin AM, Jenden DJ. Cholinesterase inhibition improves blood flow in the ischemic cerebral cortex. Brain Res Bull. 1997; 42:59–70. [PubMed: 8978935]

18. Wigness BD, Dorman FD, Rohde TD, Buchwald H. The spring-driven implantable pump. A low cost alternative. ASAIO J. 1992; 38:M454–M457. [PubMed: 1457901]
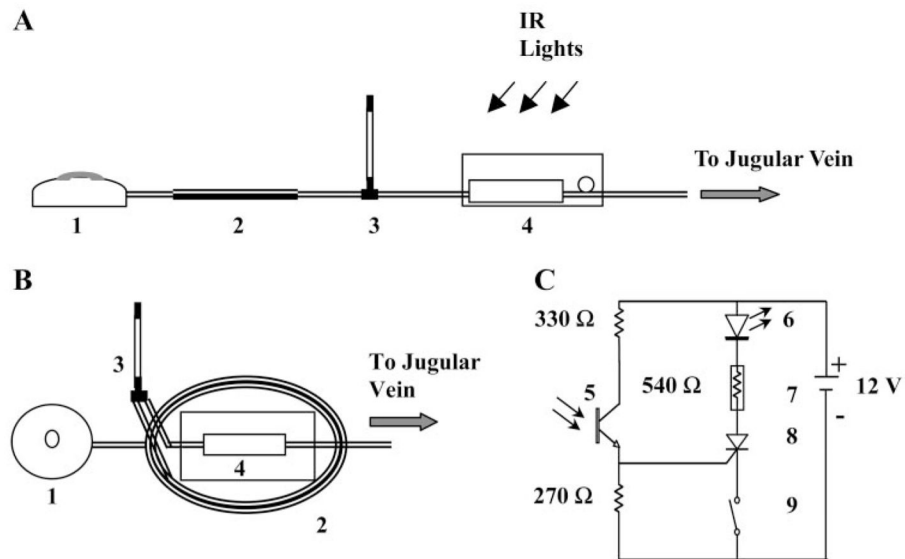
Fig. 1.

Design of the microbolus infusion pump (MIP). *A*: components consist of a reservoir (*1*), an ejection chamber (*2*), a percutaneous T tube (*3*), and an electronic module (*4*). *B*: MIP assembly: the ejection chamber (*2*) consists of a coil of tubing, on top of which is mounted the electronic module (*4*). *C*: the circuit schematic of the electronic module depicting the battery source, resistors, and photosensor (*5*), light-emitting diode (LED) (*6*), solenoid valve (*7*), silicon-controlled rectifier (*8*), and REED switch (*9*). IR, infrared.
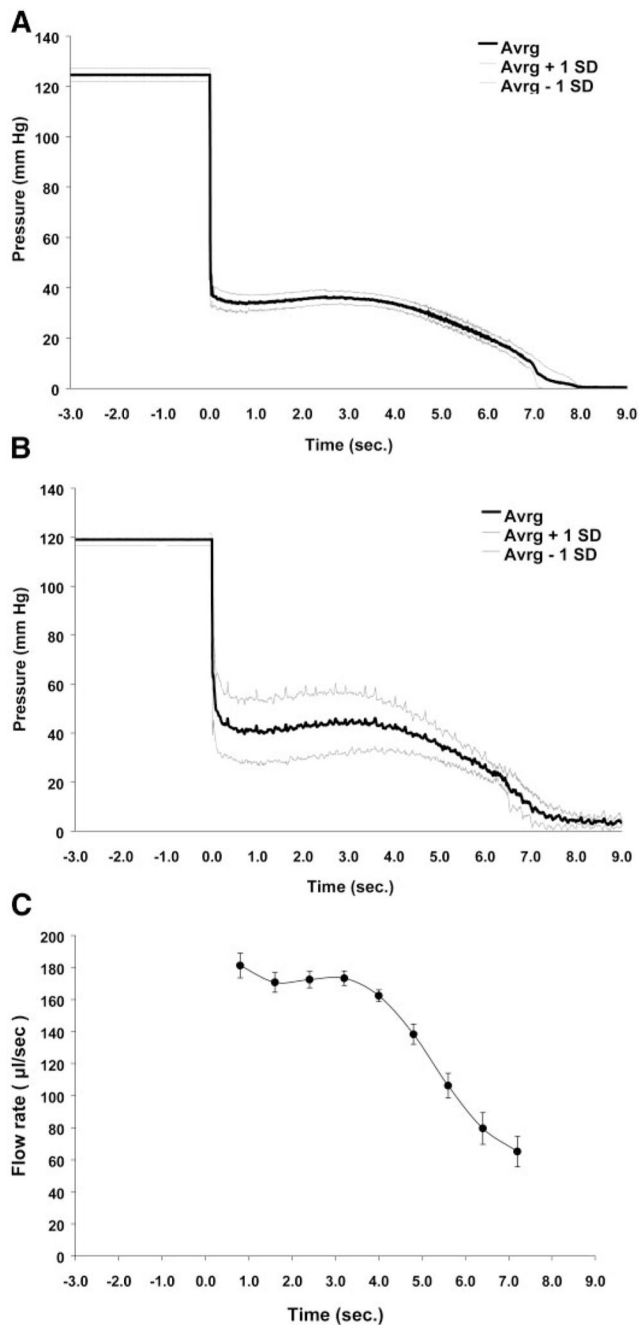
Fig. 2.
Characterization of MIP performance. *A*: change in mean pressure (±SD) over time of the MIP (*n* = 8) under ex vivo conditions. *B*: change in mean pressure (±SD) over time of the MIP (*n* = 8) under in vivo conditions. Pumps were triggered at *time 0*. Pressures were recorded posterior to the valve through the T tube catheter. Recurrent variability in SD reflects pulsations in the pressure recordings from the placement of the catheter tips within the right atria. *C*: flow rate (μl/s) over time of the MIP under ex vivo conditions (means ± SD, *n* = 8). The flow rate drops to 0 μl/s almost immediately after 7.2 s.
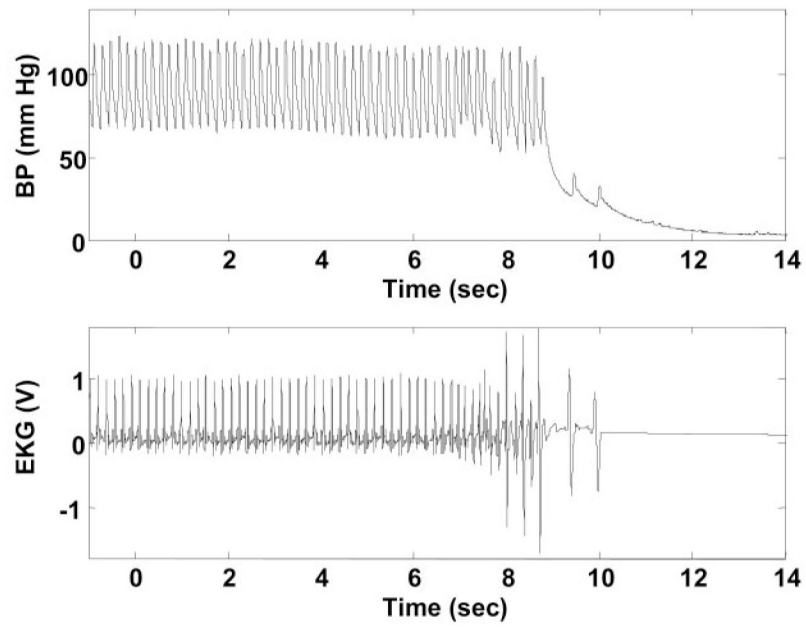
Fig. 3.
Time course of the euthanasia. Depicted is an example in an anesthetized rat of changes in femoral artery blood pressure (*A*) and cardiac rhythm (*B*) after lethal intravenous injection of 3 M KCl-pentobarbital 50 mg/kg with MIP. Triggering of the pump at *time 0* resulted after ~8 s in cardiac arrest, a precipitous drop in blood pressure (BP), and death.
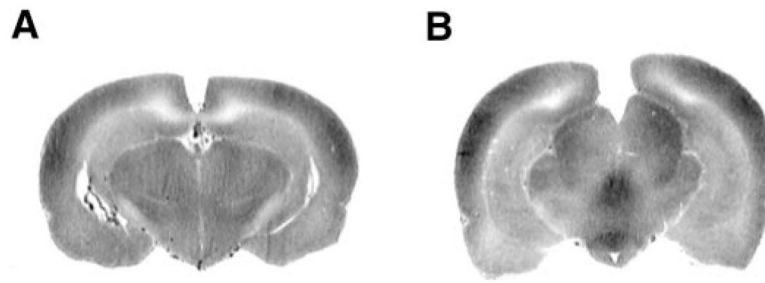
Fig. 4.
Representative iodo[^{14}C]antipyrine (AP) autoradiographs at the level of the hippocampus and lateral ventricles (*A*) (bregma AP, −4.3 mm) and interpeduncular nucleus and medial geniculate (*B*) (bregma AP, −5.8 mm). Optical densities reflect variations in regional cerebral blood flow (CBF) tracer activity.
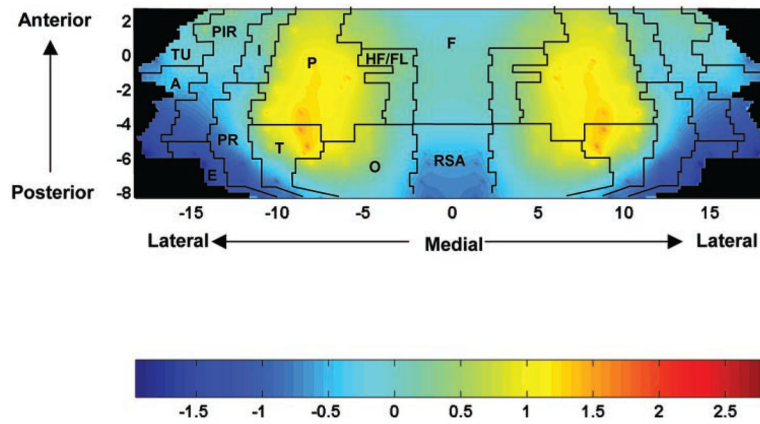
Fig. 5.
Maps of the color-coded average *Z*-scores of regional CBF tracer distribution on the two-dimensional topographic surface of the flattened cortex (*n* = 12). The *y*-axis (slices) represents coronal slices, numbered from rostral to caudal, with distance to the bregma (in mm) as labeled above (positive values being rostral to this landmark). The *x*-axis (locations) represents lateral distance from the midline (in mm) along the cortical rim within a slice. To permit easier visual correlation, we superimposed on the topographic maps the borders among the main cerebral cortical areas as defined in the anatomic atlas of Paxinos and Watson (15): A, amygdaloid; E, entorhinal; F, frontal; HF/FL, hindlimb/forelimb area; I, insular; O, occipital; P, parietal; PIR, piriform; PR, perirhinal; RSA, retrosplenial; T, temporal; TU, olfactory.